Atherosclerosis 284 (2019) 1–10

Contents lists available at ScienceDirect

Atherosclerosis

journal homepage: www.elsevier.com/locate/atherosclerosis

Nicotine-mediated autophagy of vascular smooth muscle cell accelerates atherosclerosis via nAChRs/ROS/NF-κB signaling pathway

Zhiyan Wang[1], Bei Liu[1], Jumo Zhu[1], Di Wang, Yi Wang*

Department of Cardiology, Shanghai General Hospital, School of Medicine, Shanghai Jiao Tong University, Shanghai, 200080, China

HIGHLIGHTS

- Nicotine enhances the autophagy of vascular smooth muscle cells (VSMCs) and contributes atherosclerosis.
- Autophagy induced by nicotine regulates the phenotype switching of VSMCs and subsequently functional alterations.
- The nicotinic acetylcholine receptors/ ROS /NF-κB signal pathway may involve in nicotine-induced autophagy.

ARTICLE INFO

Keywords:
Nicotine
Vascular smooth muscle cell
Autophagy
Atherosclerosis

ABSTRACT

Background and aims: Cigarette smoking is an established risk factor for atherosclerosis. Nicotine, the major constituent of cigarettes, mediates the phenotype switching of vascular smooth muscle cells (VSMCs) and contributes to atherogenesis. Recent studies show that autophagy regulates atherogenesis via several pathways. The aim of this study is to determine whether nicotine regulates autophagy and subsequently mediates the phenotypic transition of VSMCs.

Methods and results: Oil Red O and HE staining of aortic sections of *ApoE*$^{-/-}$ mice showed that nicotine promoted atherosclerosis, and *in situ* expression of α-SMA indicated the involvement of VSMCs. Western blotting documented that nicotine induced the aorta autophagy. Cultured VSMCs treated with nicotine resulted in the increase of LC3 II-to-LC3 I ratio and the decrease of P62, along with GFP-LC3 puncta assay and transmission electron microscopy, further reflecting nicotine-induced autophagy. In addition, Western blotting and quantitative real-time PCR showed that VSMCs exposed to nicotine underwent changes in the expression of differentiation markers (α-SMA, SM22α and osteopontin), confirming the role of nicotine in VSMC differentiation. Transwell migration and scratch assays demonstrated that nicotine increased the migratory capacity of VSMCs. Finally, nicotine also increased the levels of reactive oxygen species (ROS), as measured by DCFH-DA staining. After respectively inhibiting autophagy (3-MA), oxidative stress (NAC), NF-κB activity (BAY 11–7082, si-p65) and nicotinic acetylcholine receptors (nAChRs, hexamethonium), nicotine-induced autophagy and VSMC phenotype switching were reversed.

Conclusions: Nicotine-induced autophagy promotes the phenotype switching of VSMCs and accelerates atherosclerosis, which is partly mediated by the nAChRs/ROS/NF-κB signaling pathway.

1. Introduction

According to the Global Burden of Disease Study [1], ischemic heart disease is the leading cause of mortality in several developed countries, with atherosclerosis as the underlying mechanism. Vascular smooth muscle cells (VSMCs) contribute to atherogenesis following phenotype switching from the contractile to the synthetic type, which enhances their abilities to migrate and proliferate [2]. Upon migration to the intima, VSMCs also *trans*-differentiate into foam cells via CD36 upregulation and cholesterol uptake, thereby leading to atherogenesis [3].

Autophagy is a tightly-regulated process of self-digestion which helps the cell remove impaired proteins and organelles [4]. Autophagy has the important role in several diseases, such as ischemia-reperfusion, acute kidney injury and cancers [5,6]. Recent studies have shown

* Corresponding author. Department of cardiology, Shanghai General Hospital, School of Medicine, Shanghai Jiao Tong University, 100 Haining Road, Shanghai, 200080, China.
E-mail address: wangyipublic@hotmail.com (Y. Wang).
[1] These authors contributed equally to this article.

https://doi.org/10.1016/j.atherosclerosis.2019.02.008
Received 14 September 2018; Received in revised form 22 December 2018; Accepted 1 February 2019
Available online 22 February 2019
0021-9150/

evidence of autophagy in the arterial walls, which may be involved in atherogenesis [7,8]. While autophagy degrades damaged intra-cellular material to protect plaque cells against oxidative stress, it also induces formation of protein and oxidized lipid complexes known as ceroids [9], thereby facilitating atherogenesis. In addition, autophagy also exerts multiple effects on VSMCs in different conditions [10].

Nicotine is considered as the major component of cigarette smoke, a widely accepted risk factor of atherosclerosis. Nicotine has effects on several vascular cells, including the aortic endothelial cells, mast cells, macrophages and VSMCs [11–14]. The interaction between nicotine and autophagy has been discussed in current years [15,16]. However, it remains to be elucidated whether the autophagy-triggered changes in VSMCs are involved in nicotine-induced atherosclerotic lesions.

We found evidence of an atherogenic role of nicotine-induced autophagy on VSMCs. Nicotine significantly upregulated autophagy in the cultured VSMCs as well as aorta tissue with advanced atherosclerotic plaques. In addition, the nicotine-induced autophagy also induced the phenotypic transition of VSMCs via nicotinic acetylcholine receptors/reactive oxygen species/nuclear factor kappa B (nAChRs/ROS/NF-κB) signaling pathway, which subsequently promoted atherosclerosis.

2. Materials and methods

2.1. Cell culture

A mouse VSMC line (MOVAS cells, ATCC) was cultured in high-glucose Dulbecco's Modified Eagle's Medium (DMEM, Hyclone, Logan, UT, USA) with 10% fetal bovine serum (FBS, Gibco, Australia), 100U/ml penicillin and 100 μg/ml streptomycin, and placed in a humidified atmosphere of 95% air and 5% CO2 at 37 °C. The medium was changed every 2–3 days.

2.2. Reagents and chemicals

Nicotine and 3-methyladenine (3-MA) were purchased from Sigma-Aldrich (St. Louis, MO, USA), Lipofectamine 3000 from Invitrogen (USA, California), Trizol and SYBR RT-PCR Kit from Takara Bio Inc. (Japan), BAY 11–7082, rapamycin and chloroquine (CQ) and hexamethonium (HEX) from MedChemExpress (USA), and N-Acetyl-L-cysteine (NAC) from Beyotime Biotechnology (Nantong, China). Antibodies against α-SMA, SM22α, collagen I, p-p65, p65, p-IκBα, IκBα, LC3 I/II, P62, Beclin-1 and GAPDH were purchased from Cell Signaling Technology (Boston, MA, USA), and those against osteopontin from Sangon Biotech (Shanghai, CN).

2.3. Establishment of a murine atherosclerosis model

Eight-week-old *Apoe*$^{-/-}$ mice were purchased from the Cavens Animal Lab (Changzhou, China), and randomized into the following 3 groups (n = 11 per group): normal chow diet (NCD, TD08485, Harlan Teklad), high-fat diet (HFD, TD02028, Harlan Teklad), and nicotine + HFD. The latter were injected subcutaneously with 2 mg/kg nicotine daily, while the NCD and HFD groups were injected with equal volume of the vehicle. The treatment regimen lasted for 12 weeks, after which the mice were euthanatized for further analysis. All animal experiments were approved by the Animal Care and Use Committee at the Research Institute of Medicine of Shanghai Jiao Tong University. Body weight was measured weekly for all the mice. Systolic and diastolic pressure were recorded in all mice by the noninvasive tail-cuff system (CODA, Kent, USA). Plasma was collected from mice at harvest, to measure the levels of blood lipids, glucose and uric acid.

2.4. Quantitative assessment of atherosclerotic lesions

The mice were perfused through the left ventricle with normal saline, followed by 4% paraformaldehyde to fix the tissues *in situ*. The heart and aorta were dissected and embedded in paraffin, and 4 μm thick sections were cut. En face lesions at the aortic arch, thoracic aorta and abdominal aorta were stained by Oil Red O (Sigma Aldrich, Shanghai, China), and the cross-sectional lesions in the aortic root were stained with HE to evaluate the size of the atherosclerotic lesions. The areas of the cross-sectional and en face lesions were outlined using the Image Pro Plus 6.0 software, and the ratio was calculated. SMCs were evaluated by immunostaining for α-SMA (1:250, Cell Signaling Technology, USA).

2.5. Quantitative real-time PCR

Total RNA from VSMCs were isolated with TRIzol reagent according to the manufacturer's instructions (9109, Takara, Japan), and the quality and purity of the RNA were assessed using a NanoDrop-2000 spectrophotometer. Real-time PCR was performed with SYBR Green PCR Master Mix (RR036A, Takara, Japan) in an Applied Biosystems 7500 cycler. The relative mRNA levels were calculated by the $2^{-\Delta\Delta Ct}$ method, and normalized to *GAPDH*. The following primers were used: *α-SMA* forward 5′-TGTGCTGGACTCTGGAGATG-3′ and reverse 5′-GAAGGAATAGCCACGCTCAG-3′, *SM22α,* forward 5′-GATGGAACAGGCTCAAT-3′ and reverse TTCCATCGTTTTTGGTCACA-3′, osteopontin forward 5′-CAGCCATGAGTCAAGTCAGC-3′ and reverse 5′-TTGTGGCTCTGATGTTCCAG-3′, *GAPDH* forward 5′-ACTTTGTCAAGCTCATTTCC-3′ and reverse 5′-TGCAGCGAACTTTATTGATG-3’.

2.6. Transmission electron microscopy (TEM)

The electron microscopy sample as prepared as is described previously [17]. In brief, the VSMCs were treated without or with nicotine (10 μM) for 36 h, and then fixed with 2.5% glutaraldehyde, and post-fixed with 3% osmium tetroxide (OsO_4) for 2 h. The specimen was dehydrated in a graded series of ethanol, and embedded in Epon resin. For TEM study, ultrathin sections were obtained and observed using a PHILIPS CM-1220 electron microscope by the voltage of 80 kv.

2.7. GFP-LC3 puncta assay

VSMCs were transiently transfected with the GFP-LC3 plasmid to analyze the formation of autophagosomes. The transfected cells were treated with 10 μM nicotine for 36 h, washed twice with PBS, and fixed with 4% paraformaldehyde for 20 min. Images of the fluorescent puncta were obtained under a DMI3000B fluorescent microscope (Leica, Germany) equipped with the LAS V4.3 software.

2.8. Measurement of intracellular ROS generation

Intracellular ROS levels were detected using the Reactive Oxygen Species Assay Kit (Beyotime) according to the manufacturer's instructions. Briefly, the cells were seeded in 6-well plates and incubated with 10 μM nicotine for 3 h. The cells were then stained with 10 μM DCFH-DA at 37 °C in the dark for 30 min, and washed thrice with serum-free DMEM. The ROS levels were measured by flow cytometry and fluorescence microscopy.

2.9. siRNA transfection

Small interfering RNA (RNAi) against mouse p65 and corresponding scramble siRNA were synthesized by Riobio (Guangzhou, China). As previously described, VSMCs were transfected with siRNA (50 nM) via Lipofectamine 3000 (Invitrogen) according to the manufacturer's protocols before incubation with indicated agents, and harvested for further investigation.

2.10. Western blotting

See Supplemental Materials.

2.11. Transwell migration assay

See Supplemental Materials.

2.12. Scratch assay

See Supplemental Materials.

2.13. Immunofluorescence staining

See Supplemental Materials.

2.14. Statistical analysis

All data was presented as mean ± SD from at least three independent experiments. Student's *t*-test was used to compare the control and treatment groups, and multiple comparisons were performed using one-way ANOVA. p-values < 0.05 were considered statistically significant.

3. Results

3.1. Nicotine increases atherosclerotic plaque size and induces the autophagy in vivo

Apoe$^{-/-}$ mice fed a HFD for 12 weeks exhibited typical atherosclerotic lesions in the aorta, which were significantly aggravated by chronic nicotine administration via subcutaneous injection (Fig. 1A). Furthermore, nicotine treatment also increased the area of the aortic root lesions, as well as the number of SMCs in the atherosclerotic lesions after a 12-week period, although the latter was not statically significant (Fig. 1B). It also meant that VSMCs participated in the process of atherosclerosis. Nicotine administration increased the conversion of LC3 I to LC3 II but decreased the protein expression levels of P62, all of which are indicators of autophagy (Fig. 1C). Taken together, chronic nicotine aggravates atherosclerosis and promotes autophagy in the aorta.

Compared with the vehicle counterparts, body weight of mice in the nicotine group decreased significantly, which confirmed that nicotine could lead to weight loss [18]. In addition, our data showed that there was no statistical significance in lipid levels in the 2 groups (Supplemental Table 1).

3.2. Nicotine induces autophagy in cultured VSMCs

To determine the association between nicotine and autophagy in VSMCs, we firstly detected the LC3 II/I ratio and P62 expression levels in the cells. Nicotine increased the LC3 II/I ratio, decreased the protein expression of P62 and the formation of LC3 puncta in a time- and dose-dependent manner (Supplemental Fig. 1A–C); as 10 μM nicotine treatment for 36 h significantly enhanced autophagy in VSMCs, these conditions were chosen for subsequent experiments. Meanwhile, we used TEM to evaluate the autophagy levels and confirmed the effects of nicotine on autophagy of VSMCs (Fig. 1D). Since LC3 II formation is transient and LC3 II protein can be rapidly degraded by lysosomes, an increase in LC3 II could not completely represent the increasing level of autophagy. To evaluate the autophagic flux more accurately, we pretreated the cells with 10 μM chloroquine (CQ), a weak base amine that inhibits lysosomes, for 3 h to block lysosomal degradation and subsequent autophagosome degradation. Treatment of control cells with CQ increased LC3 II abundance, which was further significantly increased in cells when co-cultured with nicotine and CQ (Fig. 1E). These data indicate that nicotine may induce autophagy at the early stage of autophagosome formation. In addition to evaluating autophagy-related protein expression, VSMCs were transfected with GFP-LC3 plasmid, and the formation of LC3 puncta was monitored. There was a more significant increase in fluorescent puncta in nicotine-stimulated cells pretreated with CQ (Fig. 1F). Collectively, nicotine enhances autophagy in VSMCs.

3.3. Nicotine induces phenotype switching in VSMCs

Accumulation of numerous VSMCs in the intima indicates that atherosclerosis is predominantly a VSMC-driven disease [19], which was consistent with our *in vivo* experiments (Fig. 1B). To assess the nicotine-induced phenotypic transition of VSMCs from the contractile to the synthetic phenotype, we measured the levels of the contractile markers α-sm-actin (α-SMA) and smooth muscle protein of 22 kDa (SM22α), and the synthetic marker osteopontin [20]. Nicotine treatment for 36 h decreased the mRNA levels of *α-SMA* and *SM22α* by ~50% and upregulated osteopontin by 1.5-fold (Fig. 2B). In terms of protein expression, the abundance of α-SMA and SM22α was also decreased by 50%, while osteopontin protein levels were increased more than 2 folds following nicotine treatment (Fig. 2A). We also analyzed the expression of α-SMA by immunofluorescence assay, the results of which also showed similar trends in the protein levels (Fig. 2C).

To identify whether nicotine treatment was also responsible for the functional changes associated with the synthetic VSMC phenotype, we measured cell migration and collagen I synthesis after nicotine stimulation. Transwell and scratch wound assays showed that nicotine treatment significantly increased the migration abilities of VSMCs (Fig. 2D-E). In addition, nicotine treatment enhanced the expression of collagen I, the functional marker of the synthetic phenotype of VSMCs [21], by 2.1 folds (Fig. 2F). As a result, nicotine promotes the phenotypic switching of VSMCs from contractile to synthetic type.

3.4. Nicotine-induced autophagy mediates phenotype switching of VSMCs

To further examine whether autophagy played a role in the phenotype switching for VSMCs, we pretreated VSMCs with 3-methyladenine (3-MA, 10 mM, a PI3K inhibitor that effectively blocks autophagy), for 3 h before nicotine stimulation, and examined the contractile and synthetic protein expressions. In addition, we used rapamycin (100 nM) as positive control to induce VSMCs autophagy. There was a 3-fold increase in the fluorescent puncta in nicotine-stimulated VSMCs, and this was significantly reduced by 3-MA pre-treatment (Fig. 3A and Supplemental Fig. 2A), indicating that 3-MA inhibited the nicotine-induced autophagy in VSMCs. In addition, we found that treatment of VSMCs with 3-MA abrogated the nicotine-induced decrease in α-SMA and SM22α and increase in osteopontin (Fig. 3B). Moreover, to verify whether the inhibition of autophagy also prevented functional alterations for the synthetic phenotype of VSMCs, we also assessed the abilities of cell migration and synthesis of collagen I after nicotine treatment with or without 3-MA. We noted that 3-MA significantly prevented nicotine-mediated cell migration and collagen I synthesis (Fig. 3C–E and Supplemental Fig. 2B-C). Collectively, these results reveal that autophagy mediates nicotine-induced phenotype switching of VSMCs.

3.5. Nicotine-induced ROS generation regulate the autophagy process

Reactive oxygen species (ROS) is a vital regulator in various pathways, including autophagy [6,22]. To determine the possible role of ROS in nicotine-induced autophagy, we analyzed the amount of ROS production by nicotine stimulation by DCFH-DA staining under the fluorescence microscope and using flow cytometry. Nicotine-treated VSMCs had significantly higher levels of DCFH-DA signals compared to the control, which was alleviated by treating the cells with the

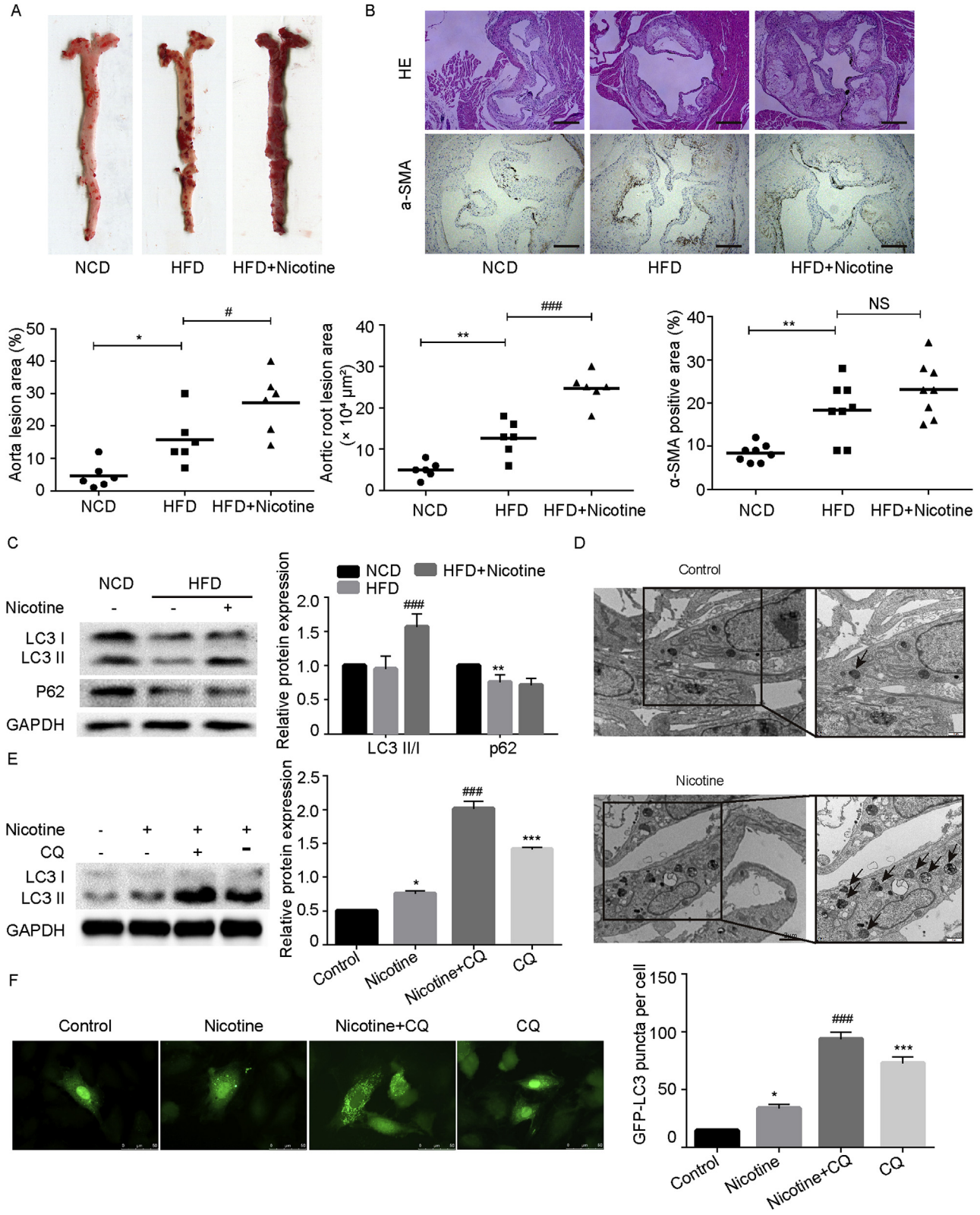

Fig. 1. Nicotine increases atherosclerotic lesion size and induces autophagy in *Apoe*$^{-/-}$ mice and VSMCs.
(A) Oil red O staining of *en face* aorta in all tested groups. N = 8. (B) Aortic bifurcations observed and photographed by hematoxylin and eosin (HE) staining and α-smooth muscle actin (α-SMA) staining of the cross sections of the aorta root. Magnification, 100×. Scale bar, 200 μm N = 8. (C) Expression of LC3 I/II and P62 in aorta tissue was quantified by Western blot. N = 3. $^{*}p < 0.05$, $^{**}p < 0.01$ and $^{***}p < 0.001$ *versus* the NCD group, $^{\#}p < 0.05$, $^{\#\#}p < 0.01$ and $^{\#\#\#}p < 0.001$ *versus* the HFD group. NS, no significance. NCD, normal chow diet, HFD, high-fat diet. (D) Transmission electron microscopy was used to evaluate autophagy induced by nicotine (10 μM, 36 h). Magnification, 24500×. Scale bar, 2 μm. The black arrows represent autolysosomes. (E) Expression of LC3 I/II and P62, and GFP-LC3 puncta assay in VSMCs pre-incubated with chloroquine (CQ, 50 μM) for 3 h before treatment with nicotine (10 μM, 36 h). Magnification, 630×. Scale bar, 50 μm. Bar graph showing the number of GFP punctae per cell. $^{*}p < 0.05$ and $^{***}p < 0.001$ *versus* the control group, $^{\#\#\#}p < 0.001$ *versus* the nicotine-treated group. N = 3.

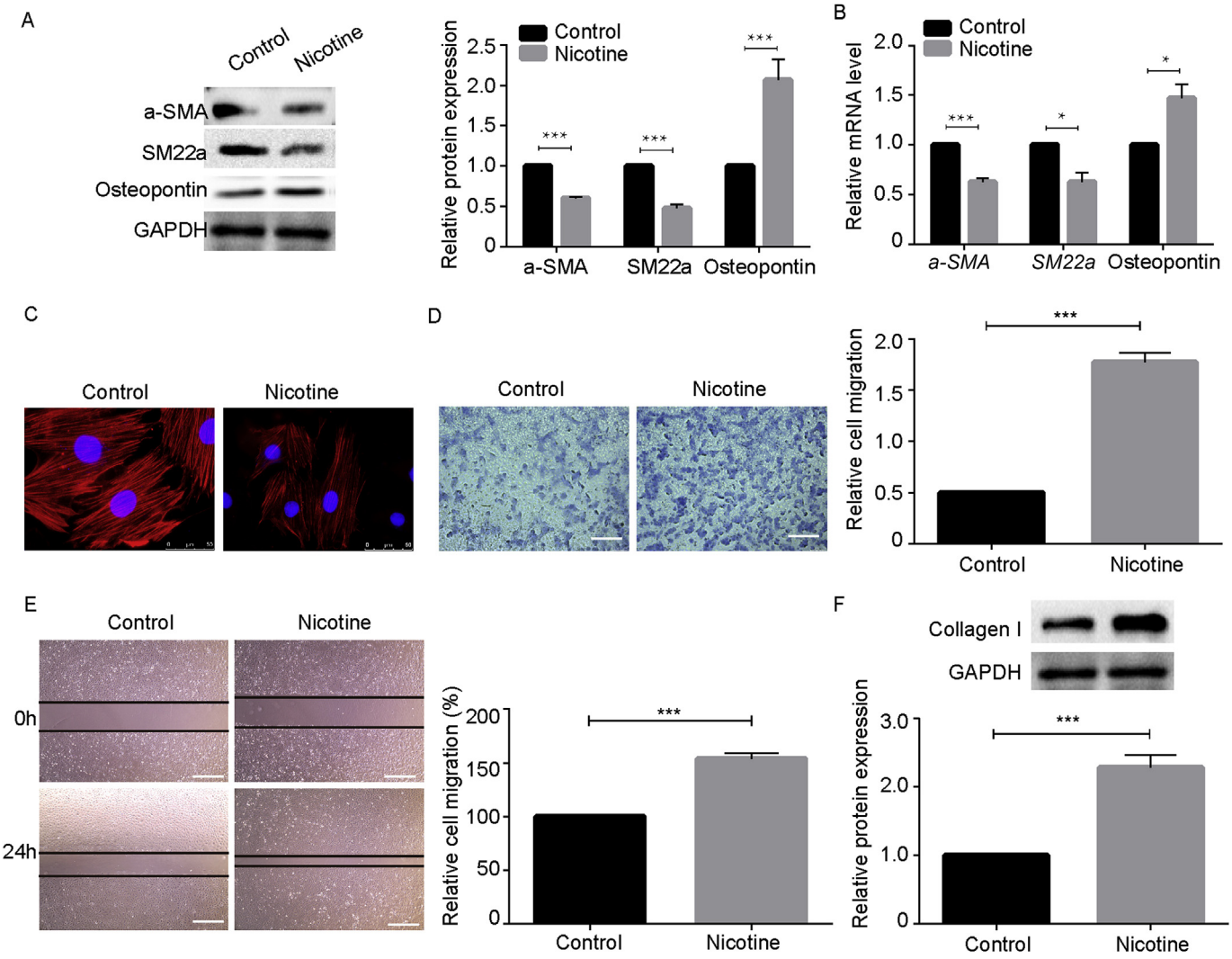

Fig. 2. Nicotine induces phenotype switching in VSMCs.
(A) Expression of α-SMA, SM22α and osteopontin after nicotine stimulation for 36 h ***$p < 0.001$ *versus* the control group. N = 3. (B) mRNA expression levels of *α-SMA*, *SM22α* and osteopontin in VSMCs treated by nicotine were quantified by quantitative real-time PCR analysis. *$p < 0.05$ and ***$p < 0.001$ *versus* the control group. N = 3. (C) Immunofluorescence images of α-SMA (red) distribution in VSMCs treated by nicotine (10 μM) for 36 h; blue staining (DAPI) indicating nuclei. Magnification, 630×. Scale bar, 50 μm N = 3. (D–E) The ability of VSMCs migration by nicotine stimulation was quantified by Transwell and scratch assays. Magnification, 100×. Scale bar, 200 μm ***$p < 0.001$ *versus* the control group. N = 3. (F) Expression of collagen I after nicotine administration. ***$p < 0.001$ *versus* the control group. N = 3.

antioxidant and ROS scavenger N-acetyl-L-cysteine (NAC) (Fig. 4A-B). These results showed that nicotine treatment promotes the generation of ROS.

To further investigate whether nicotine-induced ROS also regulated autophagy, we analyzed the level of autophagy in VSMCs treated with NAC and nicotine. We found that NAC abrogated nicotine-enhanced autophagy, both in terms of the autophagic protein levels and the formation of LC3 puncta (Fig. 4C-D and Supplemental Fig. 3A). In addition, NAC-mediated inhibition of oxidative stress was also associated with partial stabilization of α-SMA and SM22α and inhibition expression of osteopontin and collagen I (Fig. 4C), which indicated reversal of the nicotine-induced phenotype switching. Transwell and scratch wound assays showed that NAC decreased the migration ability of VSMCs induced by nicotine treatment (Fig. 4E-F and Supplemental Fig. 3B-C). Taken together, nicotine promotes ROS generation, which is essential for autophagy and phenotype switching of VSMCs.

3.6. Nicotine activates the ROS/NF-κB signaling pathway in VSMCs

ROS interacts with the NF-κB signaling pathway in multiple ways in a cell-specific manner [23]. To gain further insights into the molecular mechanism of nicotine-induced autophagy, we analyzed the effects of nicotine on the ROS/NF-κB signaling pathway. In the latent condition, IκBα is attached to the p50-p65 heterodimer complex. When IκBα is phosphorylated and subsequently degraded, phosphorylated p65 translocates to the nucleus and becomes activated [24]. VSMCs exposed to nicotine increased levels of phosphorylated p65 and IκBα (Fig. 5A). After treatment with NAC and nicotine, Western blotting analysis showed that NAC could reverse the phosphorylation of p65 and IκBα (Fig. 5A). Pre-treatment with 1 μM BAY 11–7082, the selective inhibitor of IκBα phosphorylation and the NF-κB pathway [25], for 3 h prior to nicotine stimulation, decreased the LC3 II/LC3 I ratio and the number of GFP-LC3 puncta compared to VSMCs treated only with nicotine (Fig. 5B-C). In addition, BAY 11–7082 reversed the phenotype switching by upregulating α-SMA and SM22α and downregulating osteopontin and collagen I expression (Fig. 5B). Simultaneously,

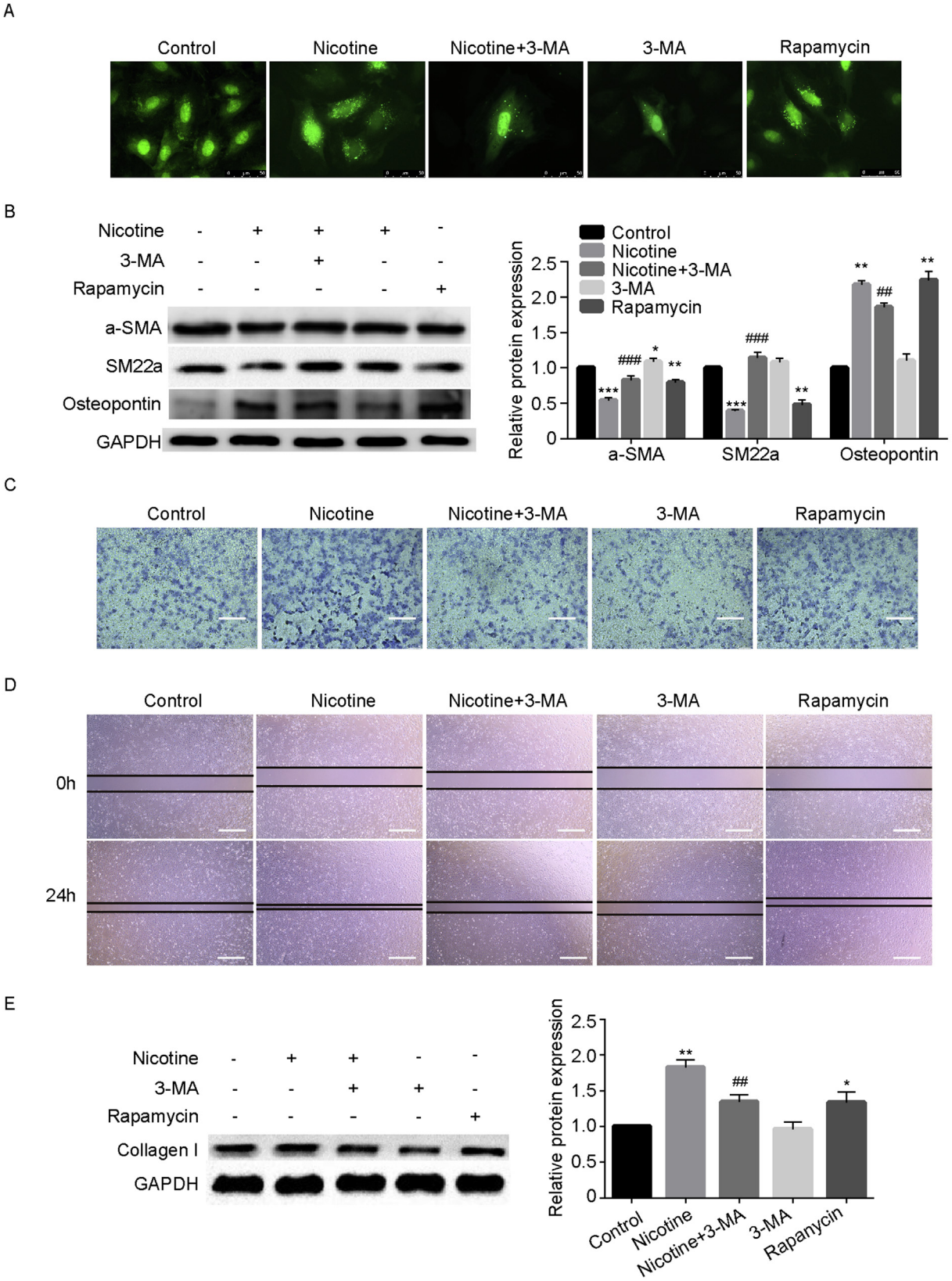

Fig. 3. Nicotine-induced autophagy is required for phenotype switching.
(A) GFP-LC3 puncta assay in VSMCs pre-incubated with 3-MA (10 mM) for 3 h before treatment with nicotine. Rapamycin (100 nM) as the positive control treated VSMCs for 36 h. Magnification, 630×. Scale bar, 50 μm. Bar graph showing the number of GFP puncta per cell for at least 10 cells per group. (B) Expression of α-SMA, SM22α and osteopontin in VSMCs pre-incubated with 3-MA (10 mM) for 3 h before treatment with nicotine. Rapamycin (100 nM) as the positive control treated VSMCs for 36 h $^{*}p < 0.05$, $^{**}p < 0.01$, $^{***}p < 0.001$ *versus* the control group. $^{\#\#}p < 0.01$ and $^{\#\#\#}p < 0.001$ *versus* the nicotine group. N = 3. (C–D) The ability of cell migration of VSMCs pretreated with 3-MA before nicotine treatment was quantified by Transwell and scratch assays. Magnification, 100×. Scale bar, 200 μm. (E) Expression of collagen I after nicotine stimulation with or without the pretreatment of 3-MA.

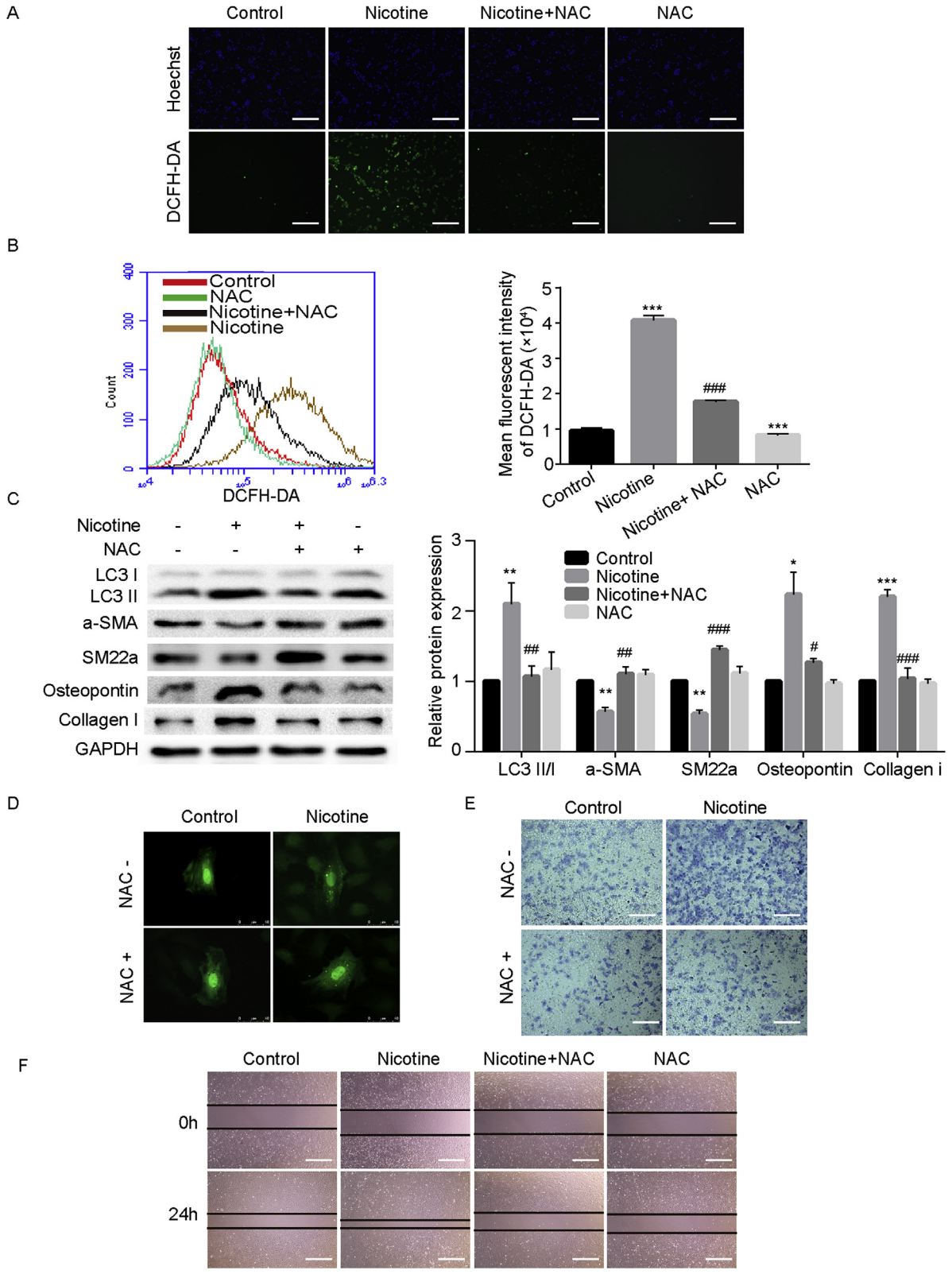

Fig. 4. Nicotine-induced ROS generation regulate the autophagy process.
(A) Staining with 10 μM DCFH-DA (green) and Hoechst (blue) of VSMCs pre-incubated with NAC before treatment with nicotine. Magnification, 100×. Scale bar, 200 μm N = 3. (B) Levels of ROS in VSMCs pre-incubated with NAC before treatment with nicotine was quantified by flow cytometry. The mean fluorescent intensity of ROS was shown in histograms. ***p < 0.001 *versus* the control group. $^{###}p < 0.001$ *versus* the nicotine group. N = 3. (C) Expression of LC3 I/II, α-SMA, SM22α, osteopontin and collagen I in VSMCs pretreated 1 mM NAC in the presence or absence of nicotine administration. $*p < 0.05$, $**p < 0.01$ and $***p < 0.001$ *versus* the control group, $^{#}p < 0.05$, $^{##}p < 0.01$ and $^{###}p < 0.001$ *versus* the nicotine-treated group. N = 3. (D) GFP-LC3 puncta assay in VSMCs pre-incubated with NAC (1 mM) for 3 h before treatment with nicotine. Magnification, 630×. Scale bar, 50 μm. Bar graph showing the number of GFP puncta per cell for at least 10 cells per group. $***p < 0.001$ *versus* the control group. $^{##}p < 0.01$ *versus* the nicotine-treated group. N = 3. (E–F) The ability of cell migration of VSMCs pretreated with NAC before nicotine treatment was quantified by Transwell and scratch assays. Magnification, 100×. Scale bar, 200 μm N = 3.

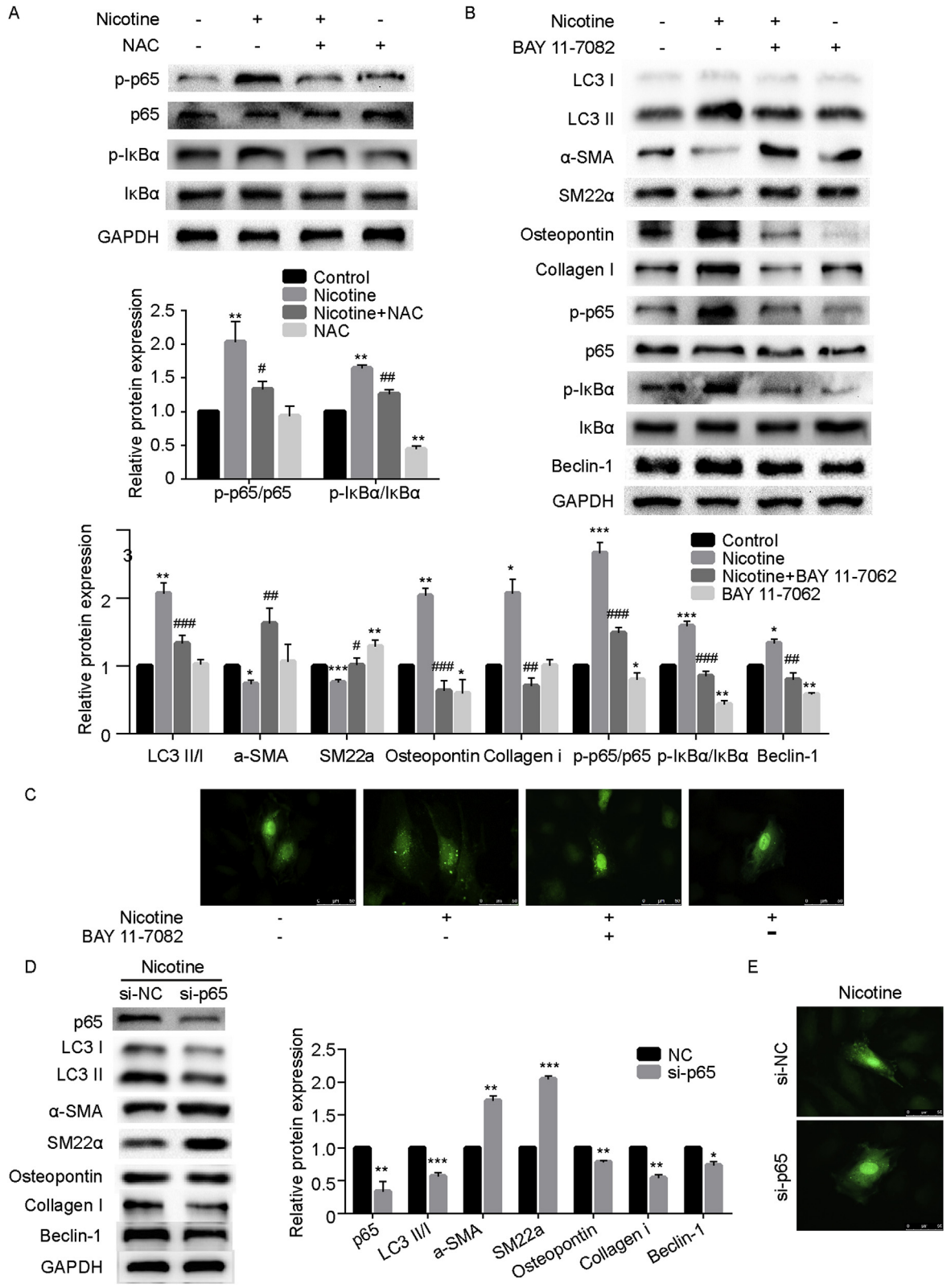

Fig. 5. Nicotine activates ROS/NF-κB signaling pathway in VSMCs.
(A) Expression of p-p65, p65, p-IκBα and IκBα in VSMCs pretreated by 1 mM NAC with the treatment of nicotine. $^{**}p < 0.01$ *versus* the control group, $^{\#}p < 0.05$ and $^{\#\#}p < 0.01$ *versus* the nicotine-treated group. N = 3. (B) Expression of LC3 I/II, α-SMA, SM22α, osteopontin, collagen I, p-p65, p65, p-IκBα, IκBα and beclin-1 in VSMCs pretreated by 1 μM BAY 11–7082 with the treatment of nicotine. $^{*}p < 0.05$, $^{**}p < 0.01$ and $^{***}p < 0.001$ *versus* the control group, $^{\#}p < 0.05$, $^{\#\#}p < 0.01$ and $^{\#\#\#}p < 0.001$ *versus* the nicotine-treated group. N = 3. (C) GFP-LC3 puncta assay in VSMCs pre-incubated with BAY 11–7082 (1 μM) for 3 h before treatment with nicotine. Magnification, 630×. Scale bar, 50 μm. (D) Expression of p65, LC3 I/II, α-SMA, SM22α, osteopontin, collagen I and beclin-1 in VSMCs transfected by si-p65 for 24 h with the treatment of nicotine. $^{*}p < 0.05$, $^{**}p < 0.01$ and $^{***}p < 0.001$ *versus* the si-nc group. (E) GFP-LC3 puncta assay in VSMCs pre-transfection with si-p65 and si-nc for 24 h before treatment with nicotine. Magnification, 630×. Scale bar, 50 μm.

treatment with si-p65 and the negative control also showed the same results (Fig. 5D-E). Furthermore, nicotine stimulation increased the expression of beclin-1 protein, the trigger protein in autophagy (Fig. 5B). The increase in beclin-1 protein was attenuated significantly in VSMCs pre-treated with BAY 11–7082 and si-p65 transfection (Fig. 5B, D). Collectively, the ROS/NF-κB pathway is involved in the nicotine-induced effects.

3.7. Nicotine regulates the autophagy process via nAChRs

To determine the receptors underlying the above process, a non-selective nicotinic acetylcholine receptor (nAChR) antagonist HEX was used. After pre-administration of HEX (10 μM) for 30 min, the effects of nicotine on VSMCs autophagy were reversed (Supplemental Fig. 4C). In addition, the levels of ROS and activation of NF-κB stimulated by nicotine also decreased by pretreatment with HEX (Supplemental Fig. 4A–C). HEX reversed the phenotype switching by upregulating α-SMA and SM22α and downregulating osteopontin and collagen I expression (Supplemental Fig. 4C). Transwell and scratch wound assays showed that HEX decreased the migration ability of VSMCs induced by nicotine treatment (Supplemental Fig. 4D-E). These findings suggest that the effects of nicotine on VSMCs are mediated through the nAChRs.

4. Discussion

Our study shows that nicotine exposure induces autophagy in VSMCs, which promotes its phenotypic transition via the nAChRs/ROS/NF-κB signaling pathway. The schematic summary of our findings is shown in Supplemental Fig. 5. This may provide novel insights into the mechanisms underlying nicotine-induced atherosclerosis.

Cigarettes contain more than 4800 chemical compounds, of which nicotine is one of the major ingredients and is considered as the main contributor to the adverse cardiovascular diseases [26]. Several vascular cells including VSMCs are involved in atherogenesis, and nicotine enhances the ability of VSMCs to migrate and proliferate [27,28], which has a crucial role in formation of the atherosclerotic plaques. The results of our *in vivo* study also revealed a similar phenomenon, further validating the effects of nicotine on atherogenesis.

Nicotine promoted phenotype switching of VSMCs from the contractile to the synthetic type, which was known to mediate atherosclerosis and plaque stability. Several studies have proposed the involvement of platelet derived growth factor, interleukin 1β and oxidized phospholipids in regulating this phenotypic transition [29–31]. Furthermore, Arany et al. found that nicotine augmented the effects of transforming growth factor-β on α-SMA and fibronectin production in proximal tubule cells, indicating that nicotine promoted the epithelial-mesenchymal transition in these cells [32]. In atherosclerosis, nicotine has also been reported as a powerful stimulant via VSMC phenotype switching [14,33], consistent with our results. Phenotype switching induces certain functional changes in VSMCs [20], such as migration and collagen synthesis, which were increased by nicotine treatment.

A previous study established the complicated connection between autophagy and phenotypic transition in VSMCs [34]. It demonstrated autophagy could be the major proteolytic process employed by the cells to remove contractile proteins [34]. Autophagy is a complex catabolic process that degrades cytoplasmic components via the lysosomes [35]. In the early stage of atherogenesis, autophagy activation may prevent plaque cells against cellular distress, especially oxidative injury, by removing abnormal organelles and protein aggregates. However, with the progression of atherosclerosis, autophagy is either excessively stimulated or impaired, leading to cell death and plaque instability [36]. Previous studies have reported that numerous factors regulate autophagy in VSMCs, such as oxidized low density lipoprotein, platelet-derived growth factor and secreted protein sonic hedgehog [34,37,38]. Our findings showed that nicotine could activate autophagy in VSMCs in a dose- and time-dependent manner. In addition, we found that nicotine-induced autophagy mediated VSMC phenotype switching by treatment with the autophagy inhibitor 3-MA, consistent with a previous study [34]. Simultaneously, the related functions of synthetic VSMCs were also regulated by autophagy. This elucidated that nicotine regulated phenotype switching of VSMCs through the autophagic process.

Nicotine, binding to nAChRs, induces several pathological changes in VSMCs [14,28]. In our studies, pretreatment with HEX (non-selective nAChRs antagonist) had inhibitory effects on nicotine-induced autophagy. Kim et al. found that nicotine caused apoptosis in renal proximal tubular epithelial cells by inducing ROS generation and acitivating NF-κB by nAChRs [39,40]. Consistent with this, our study found that nicotine-induced autophagy was reversed by the ROS scavenger NAC, indicating that the oxidative stress was an upstream mechanism for autophagy activation mediated by nicotine. Additionally, excessive ROS can activate NF-κB and further exacerbate the inflammatory response [41,42]. Our findings suggested that NF-κB proteins were downstream of ROS since NAC inhibited nicotine-induced IκBα and p65 phosphorylation. Furthermore, studies have pointed out an association between NF-κB and autophagy in several diseases [43]. Copetti et al. considered that NF-κB induced autophagy by transactivating the autophagy-triggering protein beclin-1, the promoter of which was the newly identified κB site [44]. We found that nicotine slightly increased the expression of beclin-1. Furthermore, the inhibition of NF-κB signaling pathway by the pharmacological inhibitor reversed the expression of beclin-1 and reduced autophagy induced by nicotine. As well, we used si-RNA of p65 to confirm the above effects, proved that nicotine could induce autophagy by activating the NF-κB signaling pathway. Taken together, the nAChRs/ROS/NF-κB signaling pathway is involved in nicotine-induced autophagy and related effects in VSMCs. However, the subunits of nAChRs underlying the above process were not found in our study. Clearly, further studies are needed to identify the subunits underlying these processes.

4.1. Conclusion

Our study has demonstrated that nicotine promotes atherogenesis by inducing VSMC autophagy and phenotype switching through the nAChRs/ROS/NF-κB signaling pathway. These findings provide novel insights into the understanding of the underlying mechanism of atherogenesis induced by nicotine. Further studies are required to dissect the molecular mechanisms by which nicotine enhances the autophagic program and to perform the related animal studies.

Conflicts of interest

The authors declared they do not have anything to disclose regarding conflict of interest with respect to this manuscript.

Financial support

This study was supported by 81470471 from the National Natural Science Foundation of China (NSFC) and 2018C04 from the Clinical Research Innovation Plan of Shanghai General Hospital (CTCCR).

Appendix A. Supplementary data

Supplementary data to this article can be found online at https://doi.org/10.1016/j.atherosclerosis.2019.02.008.

References

[1] Global, regional, and national age-sex specific all-cause and cause-specific mortality for 240 causes of death, 1990-2013: a systematic analysis for the Global Burden of Disease Study 2013, Lancet (London, England) 385 (2015) 117–171.

[2] C.P. Mack, Signaling mechanisms that regulate smooth muscle cell differentiation, Arterioscler. Thromb. Vasc. Biol. 31 (2011) 1495–1505.
[3] H.J. Lim, S. Lee, K.S. Lee, et al., PPARgamma activation induces CD36 expression and stimulates foam cell like changes in rVSMCs, Prostag. Other Lipid Mediat. 80 (2006) 165–174.
[4] B. Levine, D.J. Klionsky, Development by self-digestion: molecular mechanisms and biological functions of autophagy, Dev. Cell 6 (2004) 463–477.
[5] D. Patschan, K. Schwarze, E. Henze, et al., Endothelial autophagy and Endothelial-to-Mesenchymal Transition (EndoMT) in eEPC treatment of ischemic AKI, J. Nephrol. 29 (2016) 637–644.
[6] G. Wang, T. Zhang, W. Sun, et al., Arsenic sulfide induces apoptosis and autophagy through the activation of ROS/JNK and suppression of Akt/mTOR signaling pathways in osteosarcoma, Free Radic. Biol. Med. 106 (2017) 24–37.
[7] M. Ouimet, Y.L. Marcel, Regulation of lipid droplet cholesterol efflux from macrophage foam cells, Arterioscler. Thromb. Vasc. Biol. 32 (2012) 575–581.
[8] B. Razani, C. Feng, T. Coleman, et al., Autophagy links inflammasomes to atherosclerotic progression, Cell Metabol. 15 (2012) 534–544.
[9] M.J. Mitchinson, Insoluble lipids in human atherosclerotic plaques, Atherosclerosis 45 (1982) 11–15.
[10] S. Tai, X.Q. Hu, D.Q. Peng, et al., The roles of autophagy in vascular smooth muscle cells, Int. J. Cardiol. 211 (2016) 1–6.
[11] K.D. Macklin, A.D. Maus, E.F. Pereira, et al., Human vascular endothelial cells express functional nicotinic acetylcholine receptors, J. Pharmacol. Exp. Therapeut. 287 (1998) 435–439.
[12] P.P. Lau, L. Li, A.J. Merched, et al., Nicotine induces proinflammatory responses in macrophages and the aorta leading to acceleration of atherosclerosis in low-density lipoprotein receptor(-/-) mice, Arterioscler. Thromb. Vasc. Biol. 26 (2006) 143–149.
[13] C. Wang, H. Chen, W. Zhu, et al., Nicotine accelerates atherosclerosis in apolipoprotein E-deficient mice by activating alpha7 nicotinic acetylcholine receptor on mast cells, Arterioscler. Thromb. Vasc. Biol. 37 (2017) 53–65.
[14] S. Yoshiyama, Z. Chen, T. Okagaki, et al., Nicotine exposure alters human vascular smooth muscle cell phenotype from a contractile to a synthetic type, Atherosclerosis 237 (2014) 464–470.
[15] X. Bai, J.A. Stitzel, A. Bai, et al., Nicotine impairs macrophage control of Mycobacterium tuberculosis, Am. J. Respir. Cell Mol. Biol. 57 (2017) 324–333.
[16] N. Duerrschmidt, A. Hagen, C. Gaertner, et al., Nicotine effects on human endothelial intercellular communication via alpha4beta2 and alpha3beta2 nicotinic acetylcholine receptor subtypes, N. Schmied. Arch. Pharmacol. 385 (2012) 621–632.
[17] I. Perrotta, The use of electron microscopy for the detection of autophagy in human atherosclerosis, Micron (Oxford, England: 1993 50 (2013) 7–13.
[18] A. Chiolero, D. Faeh, F. Paccaud, et al., Consequences of smoking for body weight, body fat distribution, and insulin resistance, Am. J. Clin. Nutr. 87 (2008) 801–809.
[19] S. Allahverdian, A.C. Chehroudi, B.M. McManus, et al., Contribution of intimal smooth muscle cells to cholesterol accumulation and macrophage-like cells in human atherosclerosis, Circulation 129 (2014) 1551–1559.
[20] M.R. Alexander, G.K. Owens, Epigenetic control of smooth muscle cell differentiation and phenotypic switching in vascular development and disease, Annu. Rev. Physiol. 74 (2012) 13–40.
[21] B. Ho-Tin-Noe, S. Vo, R. Bayles, et al., Cholesterol crystallization in human atherosclerosis is triggered in smooth muscle cells during the transition from fatty streak to fibroatheroma, J. Pathol. 241 (2017) 671–682.
[22] R. Scherz-Shouval, Z. Elazar, ROS, Mitochondria and the regulation of autophagy, Trends Cell Biol. 17 (2007) 422–427.
[23] M.J. Morgan, Z.G. Liu, Crosstalk of reactive oxygen species and NF-kappaB signaling, Cell Res. 21 (2011) 103–115.
[24] J. Napetschnig, H. Wu, Molecular basis of NF-kappaB signaling, Annu. Rev. Biophys. 42 (2013) 443–468.
[25] S. Strickson, D.G. Campbell, C.H. Emmerich, et al., The anti-inflammatory drug BAY 11-7082 suppresses the MyD88-dependent signalling network by targeting the ubiquitin system, Biochem. J. 451 (2013) 427–437.
[26] G. Siasos, V. Tsigkou, E. Kokkou, et al., Smoking and atherosclerosis: mechanisms of disease and new therapeutic approaches, Curr. Med. Chem. 21 (2014) 3936–3948.
[27] G. Di Luozzo, S. Pradhan, A.K. Dhadwal, et al., Nicotine induces mitogen-activated protein kinase dependent vascular smooth muscle cell migration, Atherosclerosis 178 (2005) 271–277.
[28] A. Cucina, A. Fuso, P. Coluccia, et al., Nicotine inhibits apoptosis and stimulates proliferation in aortic smooth muscle cells through a functional nicotinic acetylcholine receptor, J. Surg. Res. 150 (2008) 227–235.
[29] R.A. Deaton, Q. Gan, G.K. Owens, Sp1-dependent activation of KLF4 is required for PDGF-BB-induced phenotypic modulation of smooth muscle, Am. J. Physiol. Heart Circ. Physiol. 296 (2009) H1027–H1037.
[30] N.A. Pidkovka, O.A. Cherepanova, T. Yoshida, et al., Oxidized phospholipids induce phenotypic switching of vascular smooth muscle cells in vivo and in vitro, Circ. Res. 101 (2007) 792–801.
[31] M.R. Alexander, M. Murgai, C.W. Moehle, et al., Interleukin-1beta modulates smooth muscle cell phenotype to a distinct inflammatory state relative to PDGF-DD via NF-kappaB-dependent mechanisms, Physiol. Genom. 44 (2012) 417–429.
[32] I. Arany, D.K. Reed, S.C. Grifoni, et al., A novel U-STAT3-dependent mechanism mediates the deleterious effects of chronic nicotine exposure on renal injury, Am. J. Physiol. Renal. Physiol. 302 (2012) F722–F729.
[33] C. Heeschen, J.J. Jang, M. Weis, et al., Nicotine stimulates angiogenesis and promotes tumor growth and atherosclerosis, Nat. Med. 7 (2001) 833–839.
[34] J.K. Salabei, T.D. Cummins, M. Singh, et al., PDGF-mediated autophagy regulates vascular smooth muscle cell phenotype and resistance to oxidative stress, Biochem. J. 451 (2013) 375–388.
[35] N. Mizushima, M. Komatsu, Autophagy: renovation of cells and tissues, Cell 147 (2011) 728–741.
[36] B. Levine, J. Yuan, Autophagy in cell death: an innocent convict? J. Clin. Invest. 115 (2005) 2679–2688.
[37] H. Li, J. Li, Y. Li, et al., Sonic hedgehog promotes autophagy of vascular smooth muscle cells, Am. J. Physiol. Heart Circ. Physiol. 303 (2012) H1319–H1331.
[38] Z. Ding, S. Liu, X. Wang, et al., LOX-1, oxidant stress, mtDNA damage, autophagy, and immune response in atherosclerosis, Can. J. Physiol. Pharmacol. 92 (2014) 524–530.
[39] C.S. Kim, J.S. Choi, S.Y. Joo, et al., Nicotine-induced apoptosis in human renal proximal tubular epithelial cells, PLoS One 11 (2016) e0152591.
[40] X. Wu, H. Zhang, W. Qi, et al., Nicotine Promotes Atherosclerosis via ROS-NLRP3-Mediated Endothelial Cell Pyroptosis vol. 9, (2018), p. 171.
[41] H.Y. Chung, B. Sung, K.J. Jung, et al., The molecular inflammatory process in aging, Antioxidants Redox Signal. 8 (2006) 572–581.
[42] W. Cong, D. Ruan, Y. Xuan, et al., Cardiac-specific overexpression of catalase prevents diabetes-induced pathological changes by inhibiting NF-kappaB signaling activation in the heart, J. Mol. Cell. Cardiol. 89 (2015) 314–325.
[43] N. Verma, S.K. Manna, Advanced glycation end products (AGE) potently induce autophagy through activation of RAF protein kinase and nuclear factor kappaB (NF-kappaB), J. Biol. Chem. 291 (2016) 1481–1491.
[44] T. Copetti, C. Bertoli, E. Dalla, et al., p65/RelA modulates BECN1 transcription and autophagy, Mol. Cell Biol. 29 (2009) 2594–2608.